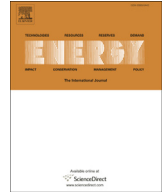




ELSEVIER

Contents lists available at ScienceDirect

Energy

journal homepage: www.elsevier.com/locate/energy

Co-optimization of energy and reserve in standalone micro-grid considering uncertainties

Salah Bahramara ^a, Pouria Sheikhhahmadi ^b, Hêmin Golpîra ^{b,*}^a Department of Electrical Engineering, Sanandaj Branch, Islamic Azad University, Sanandaj, Iran^b Department of Electrical and Computer Engineering, University of Kurdistan, Sanandaj, Iran

ARTICLE INFO

Article history:

Received 14 November 2018

Received in revised form

1 April 2019

Accepted 8 April 2019

Available online 9 April 2019

Keywords:

Renewable energy resources

Risk management

Standalone micro-grid

Stochastic programming problem

Uncertainty

ABSTRACT

The electrical energy systems suffer from several problems of operation including production of greenhouse gas emissions and low energy efficiency in fossil fuel-based power plants as well as high energy losses in transmission and distribution networks. Transition from the traditional centralized power generation into distributed power generation, via distributed energy resources, is introduced as a solution to deal with these problems. Micro-grid concept, as a cluster of distributed energy resources and local loads, is introduced to effectively realize distributed power generation. In standalone mode, micro-grid operator faces uncertainties which should be appropriately tackled into the operation problem formulation. For this purpose, a new decision making framework is proposed in this paper which guarantees optimal scheduling of distributed energy resources to simultaneously provide energy and reserve. The proposed modeling framework, which is visualized through a new risk-based stochastic approach, controls the risk of micro-grid operator in decision-making by Conditional Value at Risk method. Numerical results demonstrates the effectiveness of the proposed framework to model the operation problem of a standalone micro-grid under different uncertainties. Moreover, sensitivity analysis reveals that by increasing the percentage of invoked reserve the expected total cost of micro-grid operator increases to manage the uncertainties.

© 2019 Elsevier Ltd. All rights reserved.

1. Introduction

Technical merits of Micro-Grids (MGs) make them attractive to fulfill the increasing needs for electrical energy. MGs, as clusters of Distributed Energy Resources (DERs), could operate in standalone or grid connected modes. Aside from significant benefits of MGs, they introduce new uncertain parameters which in turn may affect MG/power system performance. This paper focuses on standalone MG operation formulation to simultaneously schedule energy and reserve with the aim of compensating for uncertainties.

1.1. Motivation

Currently, carbon dioxide (CO₂) emissions from industrial processes and fossil fuel combustion, especially in large power plants, produce 65% of the emissions [1]. Global warming, as an important environmental issue, skews policy makers attention towards low-

carbon emissions energy systems to realize the goal of sustainable development [2]. In this way, Renewable Energy Sources (RESs) are introduced as efficient and emission-free solution in power industry to supply the increasing demand [1]. This leads to energy saving as conventional power plant with about 33% efficiency would be replaced by RESs. Moreover, energy saving goal is further achievable through RESs as the demand would be locally supplied which in turn decreases network energy losses. Of note that, energy saving concept reaches maturity by introducing of MG concept.

Appropriate modeling of uncertainties is of the high importance for power system decision-makers and operators. Different approaches are used by power system decision-makers to deal with the uncertainties of demand, market prices, and network equipment failures. However, MGs, as a key players in the modern power systems, manage DERs in the associated network to locally meet the demand [3]. MGs operate in two different ways namely, grid-connected and standalone modes. In the grid-connected mode, the MG Operator (MGO) manages the effect of uncertain parameters on the energy balance by exchanging energy with the main grid. Indeed, the total operation cost of MG in grid-connected mode

* Corresponding author.

E-mail address: hemin.golpira@uok.ac.ir (H. Golpîra).

Nomenclature

Indices and sets

j, J	Index and set of generating units
t, T	Index and set of time periods
ω, W	Index and set of scenarios
R, C, I	Indices of residential, commercial, and industrial loads, respectively

Parameters

S^{DN}, S^{UP}	Maximum upward/downward variation of each type of loads (%)
e^R, e^C, e^I	Maximum interruptible load coefficients (%)
$\gamma^R, \gamma^C, \gamma^I$	Percentage of load consumption for providing reserve (%)
\bar{E}, \underline{E}	Max/Min energy stored in the ESS (kWh)
E_i, E_f	Initial/Final energy stored in the ESS (kWh)
η_{CH}, η_{DCH}	Charging/Discharging efficiency of the ESS
P_{ESS}	Maximum charging/discharging power limits (kW)
$P_{\omega,t}^{WT}$	Output power of wind turbine generation in scenario ω and period t (kW)
$P_{\omega,t}^{PV}$	Output power of solar generation in scenario ω and period t (kW)
$\bar{P}_j^{DG}, \underline{P}_j^{DG}$	Maximum/Minimum output power of DG j (kW)
RR_j^{DN}	Ramp-down of DG j (kW/min)
RR_j^{UP}	Ramp-up of DG j (kW/min)
$P_t^{D-RCI-Det}$	Deterministic load consumption in period t (kW)
$P_{\omega,t}^{D-RCI}$	Probabilistic load consumption in scenario ω and period t (kW)
SR_t	Spinning reserve requirement in period t (kW)
λ_ω	Probability of occurrence of scenario ω confidence level
α	Confidence level
β	Risk-aversion parameter
C_t^{IL-RCI}	Load interruption cost in period t (\$/kWh)
C_t^{res}	Providing reserve cost in period t (\$)
C_t^{DN-RCI}	Load shifting cost in period t (\$/kWh)

C_j	Fuel cost of DG j (\$)
$SU_{j,\omega,t}$	Start-up cost of DG j in scenario ω and period t (\$)
$SD_{j,\omega,t}$	Shut-down cost of DG j in scenario ω and period t (\$)
C_{ESS}	Charging/Discharging cost of the ESS (\$/kWh)
r_t	Percentage of reserve invoking (invoked reserve parameter) in period t (%)

Variables

ETC	Expected total cost of the micro-grid (\$)
CVaR	Conditional value at risk (\$)
η_ω	Auxiliary non-negative variable value at risk
ξ	Auxiliary variable value at risk
$P_{\omega,t}^{CH}$	Charging power of the ESS in scenario ω and period t (kW)
$P_{\omega,t}^{DCH}$	Discharging power of the ESS in scenario ω and period t (kW)
$E_{\omega,t}$	Energy stored in the ESS in scenario ω until period t (\$/kWh)
$P_{j,\omega,t}^{DG}$	Output power of DG j for supplying energy in scenario ω and period t
$R_{j,\omega,t}^{DG}$	Output power of DG j for supplying reserve in scenario ω and period t
P_t^{IL-RCI}	The amount of interruptible loads for supplying energy in period t
R_t^{IL-RCI}	The amount of interruptible loads for supplying reserve in period t
P_t^{DN-RCI}	The amount of responsive loads which shift downward in period t
P_t^{UP-RCI}	The amount of responsive loads which shift upward in period t
$U_{j,\omega,t}^{DG}$	Binary variable (=1, if DG j is online in scenario ω and period t ; = 0 otherwise)
$X_{\omega,t}^{CH}$	Binary variable (=1, if ESS is charging in scenario ω and period t ; = 0 otherwise)
$X_{\omega,t}^{DCH}$	Binary variable (=1, if ESS is discharging in scenario ω and period t ; = 0 otherwise)

is minimized using a deterministic decision-making problem which changes the load pattern and penetration level of RESs, see for example [4]. To deal with uncertainties in the operation problem of MGs, robust optimization approaches would be employed in which optimal scheduling of DERs and exchanging energy with the main grid are determined, see for example [5]. However, modeling operation problem of a standalone MG considering uncertainties is significantly different from those of grid-connected mode. In standalone mode, MGO needs appropriate decision-making frameworks for optimal scheduling of resources to manage uncertainties which is the main aim of this paper.

1.2. Literature review and contributions

This sub-section aims to review recent advances in the field of standalone MG operation. An optimal two-level approach is introduced in Ref. [6] to simultaneously minimize the operation costs and emission. While the early stage stands for providing an economic operating scheme, the later tackles technical constraints of the MG, such as voltage limits and power flow, into the problem

formulation. A real-time operation problem of an MG is formulated by a deterministic model in Ref. [7]. Binary Particle Swarm Optimization (PSO) algorithm is used to minimize energy cost and pollutant emission and to maximize the available power of RESs. Since the deterministic model is independent of scenarios, it suffers from lack of control over uncertainties. Deterministic unit commitment problem which minimizes economic cost and emission pollution without modeling uncertainties is discussed in Ref. [8]. A double-layer, including schedule and dispatch layers, coordinated control approach is proposed in Ref. [9] for MG energy management. In the schedule layer, MG operation is performed in respect of the forecasted data. Then, generated power of dispatchable units are determined according to the real-time data in the dispatch layer. An optimal control scheme based on combined dispatch strategies is developed to realize the minimal operation cost of MG [10]. A mixed integer programming is derived in Ref. [11] for optimal operation of a standalone DC MG, in which the model is deterministic and MGO cannot control uncertain parameters and manage risk. A multi-objective linear programming methodology is proposed in Ref. [12] to determine the operating points of various

- In the studies, the operation problem of MG is modeled using deterministic and probabilistic approaches. In the early one, the uncertain parameters are not mathematically modeled in the problem and in the later, the expected of the scenarios is considered in each time-step. Moreover, different operation strategies, visualized by dispatchable DERs, are introduced to cover the uncertainties. Generally, the so far researches could not model risk of MGO decisions.

The present paper aims to overcome the above crudities by simultaneous modeling of energy and reserve. Therefore, the main contributions of this paper are twofold:

- 1) Proposing a new mathematical model in which the problem of energy scheduling of DERs is jointly optimized with the problem of reserve scheduling of the resources. Of note that reserve is formulated to model uncertainties of equipment failures or unpredicted events.
- 2) Proposing a risk-based two-stage stochastic optimization approach to model the uncertain behavior of RESs and demand in the operation problem of a standalone MG and controlling the risk level of MGO in decisions by Conditional Value at Risk (CVaR) method. The uncertainties of the parameters are modeled by generating different scenarios using the associated Probability Distribution Functions (PDFs). The first-stage output, preceding the occurrence of operation scenarios, is optimal

contracts with loads to interrupt and shift for energy management and interrupt for reserve management. On the other hand, optimal scheduling of DGs and ESSs for energy purpose and optimal dispatching of DGs for reserve purpose, followed by occurrence of scenarios, are considered as the second-stage decisions in real-time operation.

2. Problem description

Two main approaches are mathematically formulated to tackle the uncertainties with known and unknown PDFs into standalone MG operation problem. In the early one, 24000 scenarios are generated based on normal, weibull, and irradiance distribution models, which are used as PDFs of demand, wind speed, and solar radiation, to model uncertainties of electricity demand and power generation of RESs. GAMS/SCENRED package and fast-forward scenario reduction technique are used to reduce the generated scenarios to 15 scenarios. Each scenario consists of wind speed, solar radiation, and load consumption data for the time period of operation. In the later, to appropriately model the uncertainties with unknown PDFs, such as unpredicted events, an indicated amount of reserve is considered. The developed framework is a risk-based two-stage stochastic optimization approach in which the energy and reserve scheduling of DERs is optimized simultaneously. Details of the framework is illustrated in Fig. 1 and described in what follows.

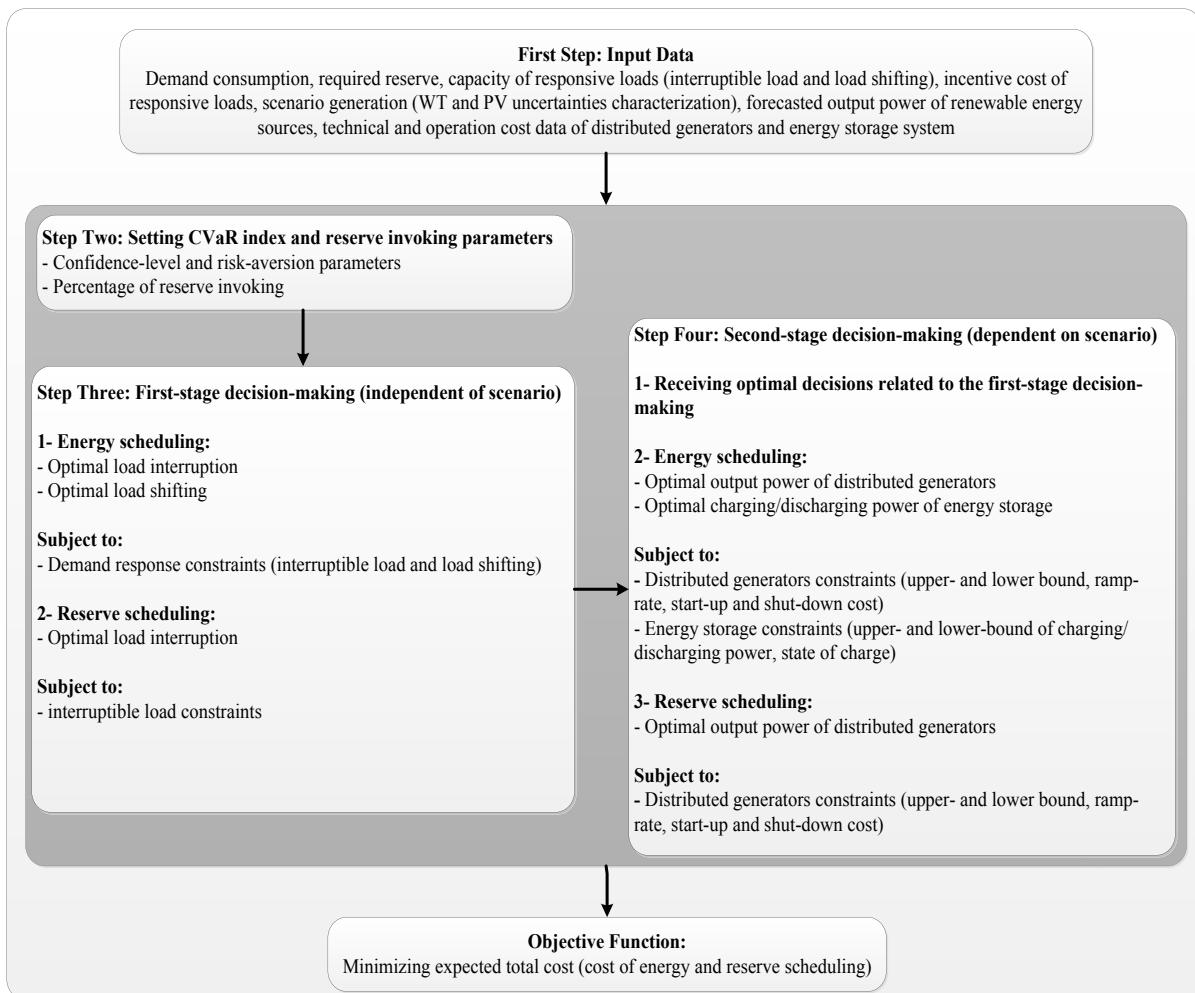


Fig. 1. Two-stage stochastic decision-making structure for MG energy and reserve scheduling.

- Step 1 Specification of input data. The model requires several input data, including demand consumption, technical and economical characteristics of resources, forecasted output power of RESs as well as generated scenarios to model the associated uncertainties, and the required reserve.
- Step 2 Setting CVaR index and reserve invoking parameters. In the developed framework, total cost of the MG operation can be manipulated by the risk-aversion and invoked reserve parameters.
- Step 3 First-stage decision-making. Since the MGO signs contracts with responsive loads to curtail or shift the associated loads in the previous day of real operation, these decisions do not depend on realization of stochastic process and are considered as the first-stage or here-and-now decisions.
- Step 4 Second-stage decision-making. Power generation of DGs and power charging/discharging of batteries which depends on realization of each scenario are considered as the second-stage or wait-and-see decisions. Moreover, interruptible loads and DGs are considered as the two resources in the first- and the second-stage decisions, respectively, which can provide the required reserve for the MGO.

Of note that the decision variables of both the first- and second-stages are determined considering the associated technical constraints (see Fig. 1). Objective function is formulated according to minimization of expected total cost of energy and reserve of step 3 and step 4.

3. Problem formulation

The operation problem of the MG is formulated as the following stochastic mathematical model:

3.1. Hypotheses

Two key assumptions are introduced in the proposed framework to model operation of a standalone MG, namely:

- The same reasoning that is used in Wien Automatic System Planning (WASP) software to formulate generation expansion planning can be extended to formulate standalone MG operation problem. In this way, all the resources and demand, associated with the MG, are connected to the main bus in the low voltage distribution network. In this way, the power losses of the low voltage network and the actual demand of the MG are aggregated in the demand of the MG which may be forecasted by the MGO and supplied by MG's resources. Therefore, in this paper, grid of MG is represented as a single-bus model and the equality constraint may be described by the balancing between power generation and demand without considering the power flow. This common assumption is also considered in several references, for example [26,29–31].
- Following the same reasoning that is used in power system operation, the amount of reserve can be determined using the maximum capacity of generation resources or as the percentage of the maximum amount of demand [32].

3.2. Expected total cost

The expected total cost (ETC) of MG which is used to simultaneously schedule energy and reserve may be formulated as:

$$ETC = \sum_{\omega \in W} \lambda_{\omega} \left[Cost_{DG}^E + Cost_{ESS}^E + Cost_{IL}^E + Cost_{DN}^E + Cost_{AV}^R + Cost_{DG}^R + Cost_{IL}^R \right] \quad (1)$$

$$Cost_{DG}^E = \sum_{t \in T} \sum_{j \in J} \left(C_j \cdot (P_{j,\omega,t}^{DG}) + SU_{j,\omega,t} + SD_{j,\omega,t} \right) \quad (2)$$

$$Cost_{ESS}^E = \sum_{t \in T} C_{ESS} \cdot (P_{\omega,t}^{CH} + P_{\omega,t}^{DCH}) \quad (3)$$

$$Cost_{IL}^E = \sum_{t \in T} C_t^{IL-RCl} \cdot (P_t^{IL-RCl}) \quad (4)$$

$$Cost_{DN}^E = \sum_{t \in T} C_t^{DN-RCl} \cdot (P_t^{DN-RCl}) \quad (5)$$

$$Cost_{AV}^R = \sum_{t \in T} C_t^{res} \cdot (SR_t) \quad (6)$$

$$Cost_{DG}^R = \sum_{t \in T} \sum_{j \in J} C_j \cdot (R_{j,\omega,t}^{DG}) \cdot r_t \quad (7)$$

$$Cost_{IL}^R = \sum_{t \in T} C_t^{IL-RCl} \cdot (R_t^{IL-RCl}) \cdot r_t \quad (8)$$

In the proposed model, Eq. (1), as a stochastic model, describes the ETC of MG to provide energy and reserve. Eqs. (2) and (7) define costs of output power of DGs for supplying energy and reserve, respectively. Eq. (3) shows charging and discharging cost of ESS. Eqs. (4) and (8) explain cost of load interruption, defines by bilateral contracts, to supply energy and reserve. Eq. (5) describes cost of load shifting, defines by bilateral contract, to supply energy. Eq. (6) defines fixed cost of MG to provide the required reserve which may be invoked in each time period.

3.3. Risk management

Risk management method is employed to control undesired effects of uncertainties. Several risk measures, including expected shortage, variance, value-at-risk, CVaR, are introduced in the literature to make a trade-off between expected cost and variability [31,33]. Due to the advantages of CVaR, the MGO's risk-aversion is modeled using the CVaR in this paper. The MGO's risk-aversion may influence the energy and reserve scheduling. The MGO tackles the CVaR index into the operation problem formulation and specifies a parameter means risk aversion parameter (β) to control the effect of uncertain values on the operation results in the worst scenarios as well as to improve the results of such scenarios. In the scenario-based stochastic optimization approach, the CVaR at the α confidence level ($\alpha - CVaR$) can be defined as the expected cost in the $(1 - \alpha) \times 100$ percent of the worst scenarios which is presented as follows [34]:

$$\min_{\xi, \eta_{\omega}} CVaR = \xi + \frac{1}{1 - \alpha} \sum_{\omega \in W} \lambda_{\omega} \cdot \eta_{\omega} \quad (9)$$

$$TC_{\omega} - \xi - \eta_{\omega} \leq 0 \quad \forall \omega \quad (10)$$

$$\eta_{\omega} \geq 0 \quad \forall \omega \quad (11)$$

where α is the confidence level, λ_{ω} is probability of occurrence of scenario ω , TC_{ω} is the total cost of the MG in scenario ω , ξ is the

optimal value of VaR, η_ω is an auxiliary non-negative variable and considered as the excess of cost in scenario ω over ξ . Of note that the excess is positive.

3.4. Objective function

The objective of the model is to minimize the summation of cost of MG over a given time and scenarios and the CVaR value of cost multiplied by a risk-aversion parameter (β). Therefore, one could write the objective function as:

$$\min \text{ETC} + \beta \text{CVaR} \quad (12)$$

where β represents the risk-aversion parameter. When β is equal to zero, the MGO is a risk-neutral decision maker. The MGO becomes more risk-averse as β increases.

3.5. Power balance constraint

Power balance constraint of (13) guarantees the balance between total generation, including the output power of DGs, wind turbines, solar panels, discharging power of ESS (Eq. (14)), the interruptible loads (Eq. (15)), and the loads that will be shifted down (Eq. (16)), and total load consumption, including residential, commercial, and industrial loads (Eq. (17)), charging power of ESS (Eq. (14)) and the loads that will be shifted up (Eq. (18)), in period t and for scenario ω . Accordingly, power balance constraint could be explained as:

$$\sum_{j \in J} P_{j,\omega,t}^{DG} + P_{\omega,t}^{WT} + P_{\omega,t}^{PV} + P_t^{LL-RCI} + P_t^{DN-RCI} = P_{\omega,t}^{ESS} + P_{\omega,t}^{D-RCI} + P_t^{UP-RCI} \quad \forall \omega, t \quad (13)$$

where

$$P_{\omega,t}^{ESS} = P_{\omega,t}^{CH} - P_{\omega,t}^{DCH} \quad \forall \omega, t \quad (14)$$

$$P_t^{LL-RCI} = P_t^{LL-R} + P_t^{LL-C} + P_t^{LL-I} \quad \forall t \quad (15)$$

$$P_t^{DN-RCI} = P_t^{DN-R} + P_t^{DN-C} + P_t^{DN-I} \quad \forall t \quad (16)$$

$$P_{\omega,t}^{D-RCI} = P_{\omega,t}^{D-R} + P_{\omega,t}^{D-C} + P_{\omega,t}^{D-I} \quad \forall \omega, t \quad (17)$$

$$P_t^{UP-RCI} = P_t^{UP-R} + P_t^{UP-C} + P_t^{UP-I} \quad \forall t \quad (18)$$

3.6. Dispatchable distributed generation unit constraints

The operational modeling of DGs should be done according to:

- Output power constraints: Eqs. (19) and (20) describe the upper and lower bounds of DGs output power ($U_{j,\omega,t}^{DG}$ as a binary variable, specifies the operating state of DGs; 1 shows that the respective DG is on and 0 stands for vice versa). Furthermore, Eq. (21) explains the limitations of DGs for providing the required reserve.

$$P_{j,\omega,t}^{DG} + R_{j,\omega,t}^{DG} \leq \bar{P}_j^{DG} \cdot U_{j,\omega,t}^{DG} \quad \forall j, \omega, t \quad (19)$$

$$U_{j,\omega,t}^{DG} \cdot P_j^{DG} \leq P_{j,\omega,t}^{DG} \quad \forall j, \omega, t \quad (20)$$

$$0 \leq R_{j,\omega,t}^{DG} \quad \forall j, \omega, t \quad (21)$$

- Ramp rate constraints: Eq. (22) defines the dynamic behavior of DGs in compliance with ramp rate; Eq. (23) affects increasing of output power of DGs to provide required reserve.

$$-RR_j^{DN} \leq P_{j,\omega,t}^{DG} - P_{j,\omega,t-1}^{DG} \leq RR_j^{UP} \quad \forall j, \omega, t \quad (22)$$

$$R_{j,\omega,t}^{DG} \leq RR_j^{UP} \quad \forall j, \omega, t \quad (23)$$

3.7. Energy storage system constraints

The following equations describe the operational constraints of ESS [26]:

- Power charge and discharge constraints: Eqs. (24) and (25) explain the lower and upper bounds of charging/discharging process.

$$0 \leq P_{\omega,t}^{CH} \leq \bar{P}_{ESS} \cdot X_{\omega,t}^{CH} \quad \forall \omega, t \quad (24)$$

$$0 \leq P_{\omega,t}^{DCH} \leq \bar{P}_{ESS} \cdot X_{\omega,t}^{DCH} \quad \forall \omega, t \quad (25)$$

- Energy constraints: Eqs. (26) and (27) define the dynamic behavior of ESS during time interval of interest and, the minimum/maximum stored energy in ESS, respectively.

$$E_{\omega,t+1} = E_{\omega,t} + \left(P_{\omega,t}^{CH} \cdot \eta_{CH} \right) - \left(\frac{P_{\omega,t}^{DCH}}{\eta_{DCH}} \right) \quad \forall \omega, t < T \quad (26)$$

$$\underline{E} \leq E_{\omega,t} \leq \bar{E} \quad \forall \omega, t \quad (27)$$

- Initial and final stored energy in energy storage: Eq. (28) reveals that the charging and discharging of ESS should be determined in such a way that the initial and final stored energy are equal.

$$E_{\omega,i} = E_{\omega,f} = 0.3 \times (\bar{E}) \quad \forall \omega, i = 1, f = 24 \quad (28)$$

- Coordination of charging and discharging operation of energy storage: Eq. (29) assures that the charging and discharging process of the ESS does not happen simultaneously.

$$X_{\omega,t}^{CH} + X_{\omega,t}^{DCH} \leq 1 \quad \forall \omega, t \quad (29)$$

At each period t , the ESS can operate in both charging and discharging modes. Therefore, the coordination rule is governed by the binary variables $X_{\omega,t}^{CH}$ and $X_{\omega,t}^{DCH}$.

3.8. Interruptible load constraints

The MG operation problem, including bilateral contracts with each type of loads (residential, commercial, and industrial) and in the form of incentive in the first-stage decision-making, aims to supply energy and reserve in period t . The constraints of the

interruptible loads are described as:

$$0 \leq P_t^{LL-R} + R_t^{LL-R} \leq \epsilon^R \cdot P_t^{D-R-Det} \quad \forall t \quad (30)$$

$$0 \leq P_t^{LL-C} + R_t^{LL-C} \leq \epsilon^C \cdot P_t^{D-C-Det} \quad \forall t \quad (31)$$

$$0 \leq P_t^{LL-I} + R_t^{LL-I} \leq \epsilon^I \cdot P_t^{D-I-Det} \quad \forall t \quad (32)$$

3.9. Load shifting constraints

Another mechanism to realize demand response is load shifting from peak-load time to low-load time to flatten the load profile. This mechanism, which could be visualized through a bilateral contracts, would be formulated as an incentive in the first-stage decision-making of the proposed model. The associated constraints related to residential, commercial, and industrial loads are given as:

$$0 \leq P_t^{DN-R} \leq S^{DN-R} \cdot P_t^{D-R-Det} \quad \forall t \quad (33)$$

$$0 \leq P_t^{DN-C} \leq S^{DN-C} \cdot P_t^{D-C-Det} \quad \forall t \quad (34)$$

$$0 \leq P_t^{DN-I} \leq S^{DN-I} \cdot P_t^{D-I-Det} \quad \forall t \quad (35)$$

$$0 \leq P_t^{UP-R} \leq S^{UP-R} \cdot P_t^{D-R-Det} \quad \forall t \quad (36)$$

$$0 \leq P_t^{UP-C} \leq S^{UP-C} \cdot P_t^{D-C-Det} \quad \forall t \quad (37)$$

$$0 \leq P_t^{UP-I} \leq S^{UP-I} \cdot P_t^{D-I-Det} \quad \forall t \quad (38)$$

$$\sum_{t \in T} P_t^{DN-R} = \sum_{t \in T} P_t^{UP-R} \quad (39)$$

$$\sum_{t \in T} P_t^{DN-C} = \sum_{t \in T} P_t^{UP-C} \quad (40)$$

$$\sum_{t \in T} P_t^{DN-I} = \sum_{t \in T} P_t^{UP-I} \quad (41)$$

Eqs. (33)–(38) describe the upper and lower bounds of the load shifting which should be shifted down and up during the time interval of interest, respectively. Eqs. (39)–(41) are formulated to control load consumptions over the whole time period, e.g., 24 h. Indeed, these constraints ensure the load shifting while maintain the total load consumption at a certain level.

3.10. Reserve scheduling constraints

In grid-connected mode, MG does not require reserve to remain secure when faces with contingencies. However, for a standalone MG, an imbalance between the production and consumption would be compensated by the scheduled reserve. The required reserve is also determined based on the percentage of load. Moreover, the probability of occurrence of disturbance in the MG and the associated impacts on the amount of invoked reserve are modeled through the invoked reserve parameter in the MGO's decisions. The constraints of the dedicated reserve for MG operation problem are:

$$R_t^R = \gamma^R \cdot P_t^{D-R-Det} \quad \forall t \quad (42)$$

$$R_t^C = \gamma^C \cdot P_t^{D-C-Det} \quad \forall t \quad (43)$$

$$R_t^I = \gamma^I \cdot P_t^{D-I-Det} \quad \forall t \quad (44)$$

$$SR_t = R_t^R + R_t^C + R_t^I \quad \forall t \quad (45)$$

$$\sum_{j \in J} R_{j,\omega,t}^{DG} + R_t^{IL-RCI} \geq SR_t \quad \forall \omega, t \quad (46)$$

Eqs. (42)–(44) are related to the amount of reserve that is defined as a percentage of the deterministic load. Eq. (45) explains the total reserve which is provided by the residential, commercial, and industrial loads. Eq. (46) represents the total interruptible loads and output power of the committed DGs to provide reserve (SR_t) in period t and for scenario ω .

3.11. Renewable energy sources modeling

- Wind Turbine: The output power of a wind turbine has uncertain behavior and depends on wind speed. The output power of wind turbine defines as [26,30]:

$$P_{t,\omega}^{WT} = \begin{cases} 0 & 0 \leq V_{t,\omega} \leq V_{ci} \\ aV_{t,\omega}^3 + bV_{t,\omega}^2 + cV_{t,\omega} + d & V_{ci} \leq V_{t,\omega} \leq V_r \\ P_r & V_r \leq V_{t,\omega} \leq V_{co} \\ 0 & V_{t,\omega} \geq V_{co} \end{cases} \quad (47)$$

where P_r is the rated output power of wind turbine; $V_{t,\omega}$, V_{ci} , V_r , and V_{co} are the forecasted wind speed, cut-in, rated, and cut-out wind speeds, respectively; and a , b , c , and d are constant parameters of the wind turbine power curve.

- Solar Panel: The output power of solar panel depends on temperature and irradiance. The output power of solar panel defines as [35]:

$$P_{t,\omega}^{PV} = \bar{P}_{STC} \cdot \frac{K_{t,\omega}^{AC}}{K_{STC}} \cdot \left(1 + k \left(T_{t,\omega}^e - T_{STC} \right) \right) \quad (48)$$

where $P_{t,\omega}^{PV}$ is the output power of solar panel at irradiance $K_{t,\omega}^{AC}$, \bar{P}_{STC} is the maximum output power under standard test conditions; K_{STC} describes the irradiance under standard test conditions; T_{STC} and $T_{t,\omega}^e$ describe the standard temperature and cell temperature, respectively; and k is a temperature coefficient.

The proposed risk-based stochastic mathematical optimization problem is modeled as a Mixed-Integer Linear Program (MILP). The model statistics are consisting of 34480 single equations, 25189 single variables, and 13680 discrete variables. The model is implemented in GAMS environment and solved by CPLEX12 solver on a 3.2 GHz Intel Core i7 processor based on a 64-bit windows 7 system with 6 GB RAM.

4. Numerical studies

This section begins with a sub-section devoted to specification of input data, will be continued by analysis of MGO decision-making framework and will be finalized by analysis of the impact of the risk-aversion and invoked reserve parameters on the decision variables of the MGO.

Table 2
Dispatchable unit parameters.

Controllable units	P_{max} (kW)	P_{min} (kW)	Marginal cost (\$/kWh)	Shut-Down cost (\$/kWh)	Start-Up cost (\$/kWh)	Ramp-Rate (kW/h)
1	410	100	0.152	2.75	5.5	200
2	410	100	0.153	2.5	5	200
3	270	50	0.166	2.25	4.5	120
4	270	50	0.165	2.3	4.6	120
5	140	25	0.185	4	8	70
6	140	25	0.187	3.75	7.5	70
7	90	20	0.267	1.8	3.6	50
8	90	20	0.269	1.75	3.5	50
9	65	15	0.297	1.4	2.8	40
10	65	15	0.299	1.42	2.85	40
11	45	10	0.246	1	2	30
12	45	10	0.267	1.02	2.05	30

4.1. Input data

Efficiency of the proposed model is investigated on a typical MG [36] with 12 dispatchable DGs (2.04 MW). DGs parameters are given in Table 2. Also, wind turbines with capacity of 0.56 MW, photovoltaic arrays with maximum power of 1.44 MW as well as an ESS with capacity of 1500 kWh are considered in the MG [26,36]. Load consumptions of the MG, including residential, commercial, and industrial demands, are shown in Fig. 2. The hourly output power of each wind turbine and solar panel are shown in Figs. 3 and 4, respectively. The ESS features, maximum load interruption, maximum load shifting, and percentage of the load consumption, defines as the required reserve, are given in Tables 3 and 4. Moreover, the probability of occurrence of 15 scenarios which are used to model the uncertain behavior of wind speed, solar radiation, and

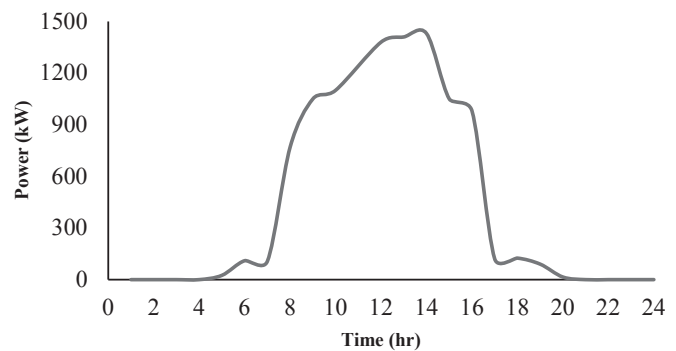


Fig. 4. Forecasted solar panel output power.

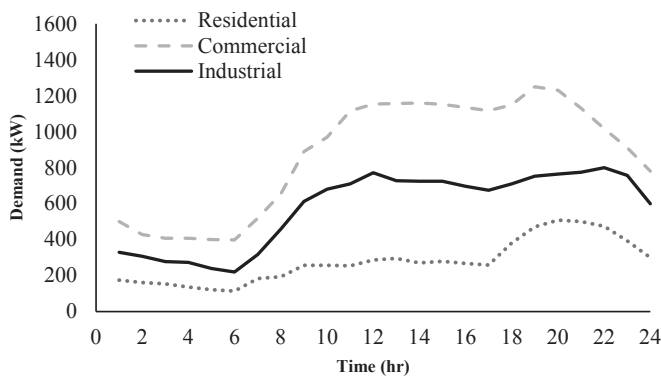


Fig. 2. Forecasted load consumption profile.

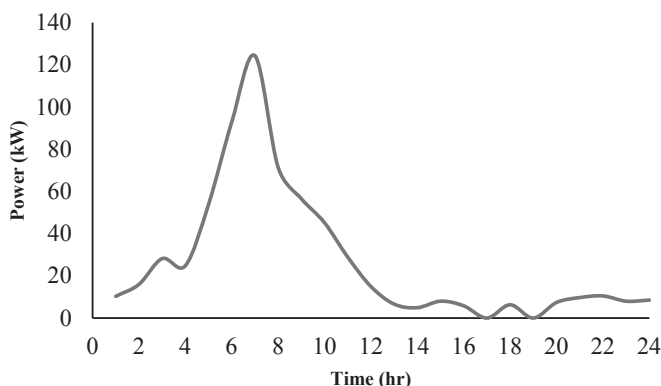


Fig. 3. Forecasted wind turbines output power.

Table 3
Characteristics of the ESS.

P_{ESS} (kW)	SOC (kWh)	SOC (kWh)	η_{CH}	η_{DCH}	C_{ESS} (\$/kWh)
400	300	1500	0.9	0.9	0.54

Table 4
The load consumption factors for determining load interruption, load shifting, and reserve.

γ^R	γ^C	γ^I	S^{DN-R}	S^{DN-C}	S^{DN-I}
10%	10%	10%	5%	5%	10%
S^{UP-R}	S^{UP-C}	S^{UP-I}	ϵ^R	ϵ^C	ϵ^I
5%	5%	10%	20%	10%	10%

Table 5
Probability of occurrence of scenarios in decision-making problem.

Number of scenario	1	2	3	4	5
Probability of scenario	0.061	0.049	0.047	0.091	0.051
Number of scenario	6	7	8	9	10
Probability of scenario	0.085	0.077	0.065	0.065	0.064
Number of scenario	11	12	13	14	15
Probability of scenario	0.074	0.087	0.067	0.063	0.054

demand are given in Table 5.

The costs of the load interruption and load shifting are shown in Figs. 5 and 6, respectively [26,37].

4.2. Results

The total operation cost of the MG in each scenario is given in

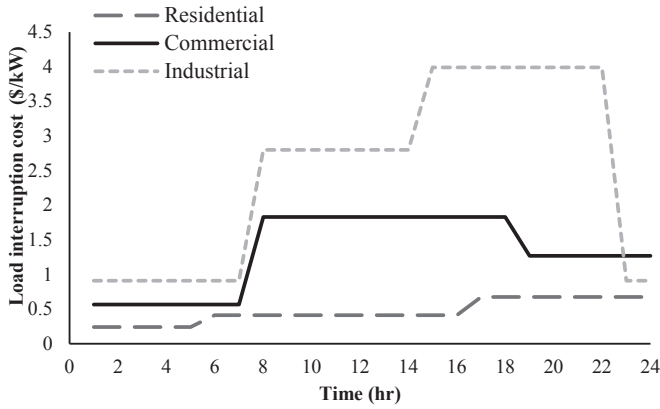


Fig. 5. Load interruption cost.

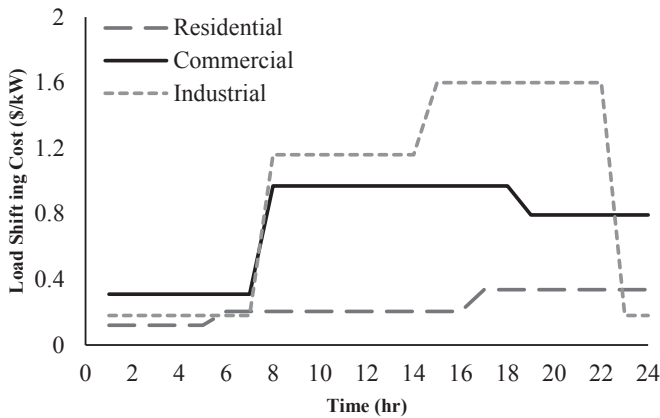


Fig. 6. Load shifting cost.

Table 6
The total cost of the MG in each scenario.

Number of scenario	1	2	3	4	5
Total Cost (\$)	8054.502	7989.446	8728.921	8595.192	7861.097
Number of scenario	6	7	8	9	10
Total Cost (\$)	7362.224	8197.298	8328.930	8427.406	8032.747
Number of scenario	11	12	13	14	15
Total Cost (\$)	8147.930	8819.463	7966.576	8728.921	7842.206

Table 6. In addition, the operation results of the MG for 24 time steps (e.g., 24 h), for the first scenario ($\omega = 1$) with risk-aversion parameter equal to 0.5, are also presented in the table. The value of α is 0.85. It means that the MGO trusts to 85% of scenarios and try to manage the remaining scenarios which are considered as the worst scenarios. Contribution of each power resources in supplying the load consumptions is shown in Fig. 7. As the operation cost of RESs is zero, considerable amount of RESs dispatched to supply load consumptions. Surplus power of RESs is delivered to the ESS at low-load hours. As the maximum dispatchable power of DGs is less than the load consumptions at hours 18–23, responsive loads and ESSs are committed to meet demand at peak load hours. Output power of DGs as well as the amount of interrupted loads, which provide reserve for the first scenario and for the probability of invoking 50% of the scheduled reserve, are shown in Fig. 8. As DGs are committed to supply the energy, load interruption is employed to supply

reserve in hours 17–23.

- First-stage decision variables (independent of scenario)

The contribution of each type of responsive loads, in compliance with the bilateral contracts between the MGO and the loads, to meet a portion of the energy and reserve are illustrated in Figs. 9 and 10. Concurrency of peak power demand with low output power of RESs in hours 17–23 justifies the maximum load interruption and load shifting in the period. The MGO specifies contribution of each type of responsive loads according to the related load interruption and load shifting cost (Figs. 5 and 6). Accordingly, the residential loads have the highest priority to be interrupted and shifted down. While, at hours 17–22, the industrial loads have the lowest contribution due to the high load interruption cost, at hour 23, industrial loads play an import role in DR program due to the low load interruption cost.

- Second-stage decision-variables (dependent on scenario): the first scenario

Results of the second-stage decision-variables, for the first scenario, are shown in Figs. 11 and 12. Fig. 11 shows the charging/discharging power and energy of the ESS. It is clear that the ESS is charged in low-load hours and committed to supply energy in peak-load hours.

Fig. 12 shows states of dispatched and non-dispatched DGs during time interval of interest. Of note that, RESs has the higher priority in decision-making of the MGO, as the DGs are accompanied with operation costs, fuel consumption cost, start-up and shut-down costs.

4.3. Sensitivity analysis

The ETC of the MG and MGO decisions are affected from the modeling of the problem and the associated parameters. Accordingly, a sensitivity analysis is performed to assess effects of mathematical model parameters, including percentage of reserve invoking, risk-aversion parameter, and percentage of load shifting, on the ETC. Results of the sensitivity analysis are shown in Figs. 13–17 and Table 7.

Fig. 13 reveals that by increasing the invoked reserve parameter, the costs of DGs and interruptible loads increase, which in turn increase the ETC. Therefore, the invoked reserve may affect MGO's decisions regarding scheduling of the energy and the reserve.

On the other hand, Fig. 14 shows that by increasing the invoked reserve parameter the DGs output power increase and the amount of load interruption decrease. This could be justified through the fact that the cost of load interruption is greater than those of DGs and the cost of probabilistic reserve invoking is included in the objective function. Therefore, using the interruptible loads to provide reserve, specifically for peak-load hours, increases the cost of the MG.

Fig. 15 represents the appraisal of the ETC versus CVaR for different values of risk-aversion parameter. It can be observed that the ETC increases and CVaR decreases as the risk-aversion parameter increases. In other words, the risk-averse operator accepts more ETC to enhance the expected cost of the worst scenarios and vice-versa for the risky operator.

Fig. 16 represents the trend of the MGO behavior, in first-stage and second-stage decisions, in response to increasing risk-aversion parameter. The results show that a risky operator relies, with the aim of achieving the lowest ETC, on the second-stage decisions. On the other hand, a risk-averse operator plays according to the first-stage decisions to control/avoid risk. This means that

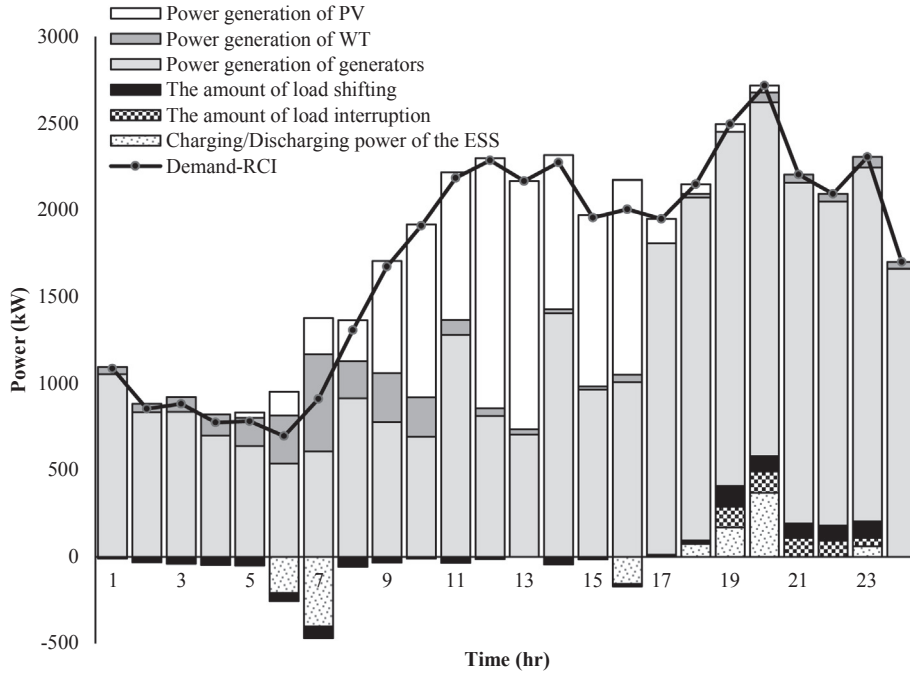


Fig. 7. Share of each power production sources to supply load consumption in the first scenario.

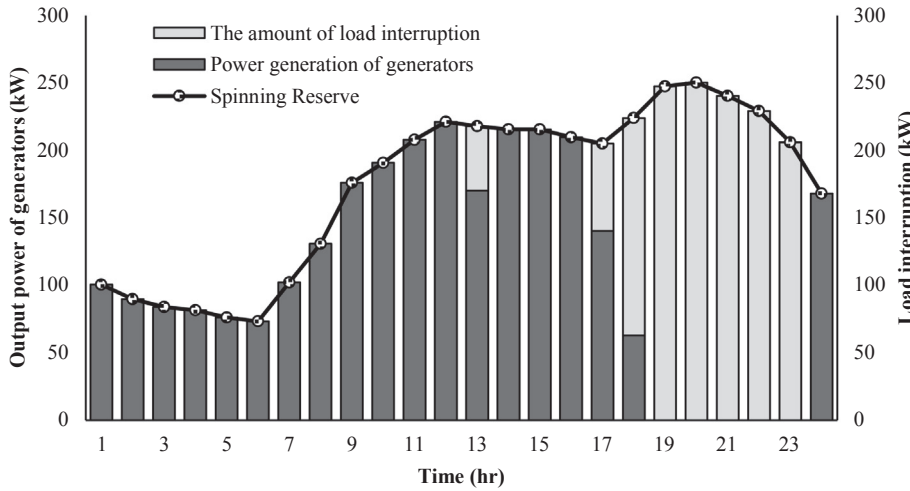


Fig. 8. Share of each DGs and interruptible loads to supply reserve in the first scenario. Also, of interest, the detailed results of the two-stage decisions are described as follows.

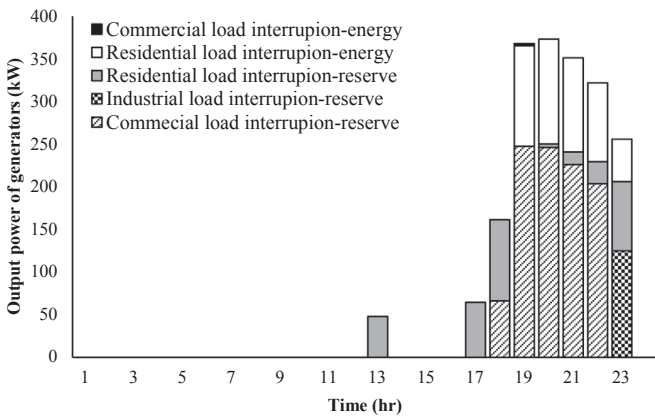


Fig. 9. Share of each type of the interruptible loads to supply part of the energy and reserve.

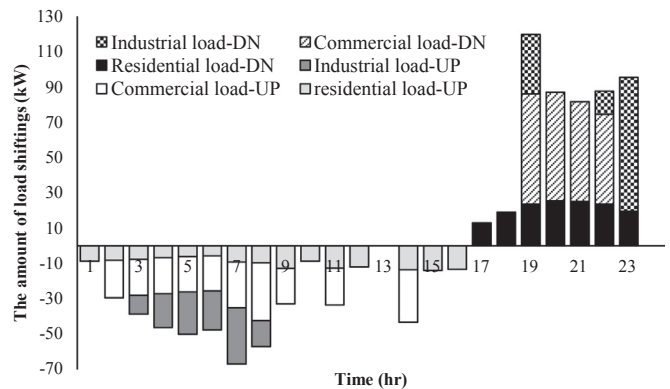


Fig. 10. Load shifting profile related to each type of load.

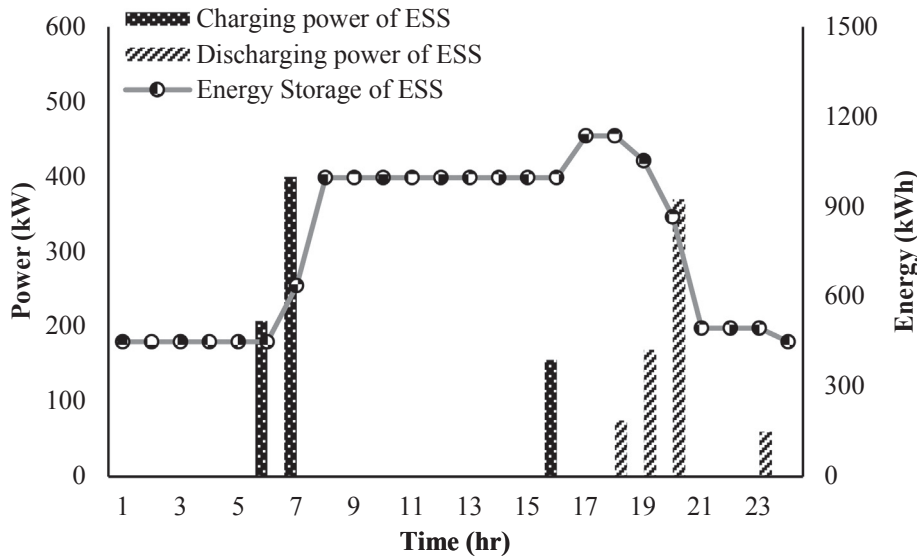


Fig. 11. Charging, discharging, and state of charge of the ESS.

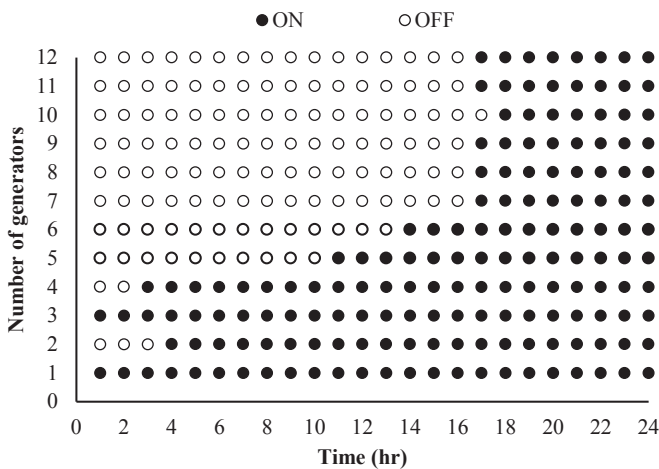


Fig. 12. State of dispatched and non-dispatched DGs.

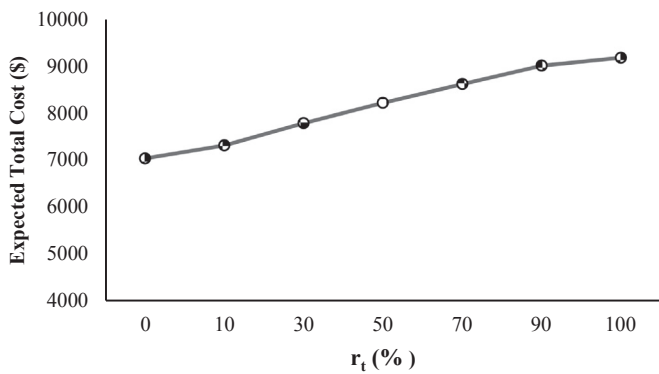


Fig. 13. Sensitivity of the ETC to percentage of reserve invoking considering $\beta = 0.5$.

$\times 100$ percent of the worst scenarios to increase.

Table 7 demonstrates the impacts of the risk-aversion and the invoked reserve parameters on the MGO's decisions. Fig. 14 reveals that by increasing the invoked reserve parameter, the first-stage decision, which meets a portion of the reserve, decreases. The results also show that by increasing the risk-aversion parameter, the output power of DGs as well as the interrupted loads, as the first-stage decisions increase. For the invoked reserve parameter of 100% and the risk-aversion parameter of 0.3, the amount of load interruption for supplying a portion of the energy decreases as it may be allocated to the scheduled reserve.

Fig. 17 shows that shifting the load consumptions from peak-load hours to low-load hours decreases the ETC. Moreover, the demand profile is more flat in comparison with the case that the load shifting approach is neglected. Therefore, DSM method is a suitable way to decrease the operation cost of MGs.

5. Conclusions

In this paper, a new approach is proposed to tackle the uncertain parameters into the operation of standalone MGs formulation. Indeed, uncertainties of equipment failures or unpredicted events are modeled by a specified reserve capacity which in turn leads to simultaneous scheduling of energy and reserve of DERs. Moreover, uncertain behavior of RESs and demand are modeled through generating different scenarios in the operation problem of MGO which could be dealt by a risk-based two-stage stochastic programming approach. Numerical results show that coordination of DERs and responsive loads decreases the ETC and guarantees the power balance constraint. Moreover, the percentage of invoked reserve has significant impact on the MGO's decisions to use various types of DERs to schedule the energy and reserve. Results show that by increasing the percentage of invoked reserve, the output power of DGs and the amount of interrupted loads, increase.

The results of sensitivity analysis reveal that the MGO determines the best decisions in compliance with the first- and second-stages to simultaneously schedule energy and reserve. Moreover, the results show that decisions of the risky operator, considering uncertainties, increase the difference between the worst and the best scenarios. On the other hand, the risk-averse operator increases the amount of interruptible loads and shifted

reliance on the first-stage decisions makes the ETC to increase while the CVaR declines. On the other hand, reliance on the second-stage decisions makes CVaR or the expected cost in the $(1 - \alpha)$

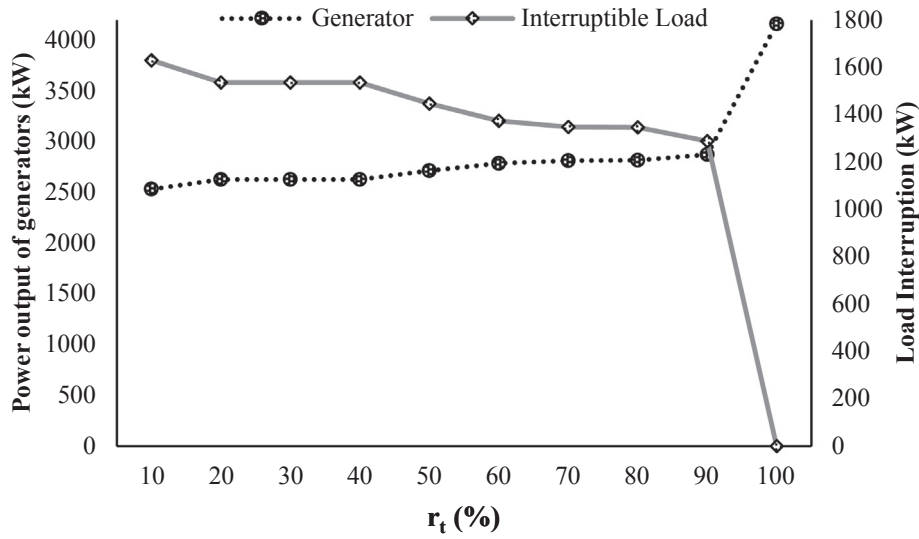


Fig. 14. Sensitivity of load interruption and DGs output power to percentage of reserve invoking considering $\beta = 0.5$.

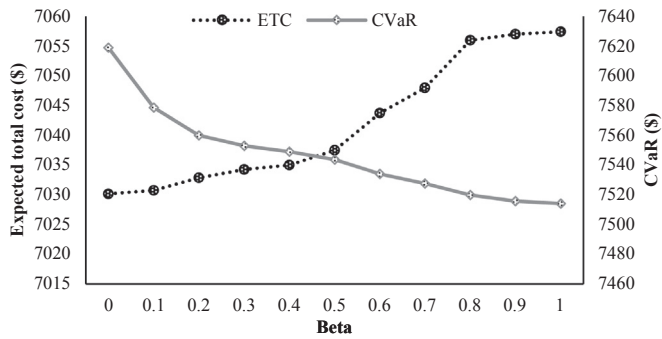


Fig. 15. Sensitivity of the ETC and CVaR to risk-aversion parameter considering $r_t = 0\%$.

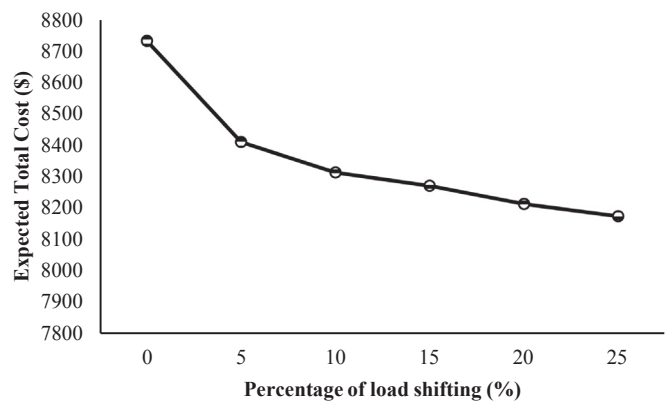


Fig. 17. Sensitivity of the ETC to percentage of load shifting ($\beta = 0.5$, $r_t = 50\%$).

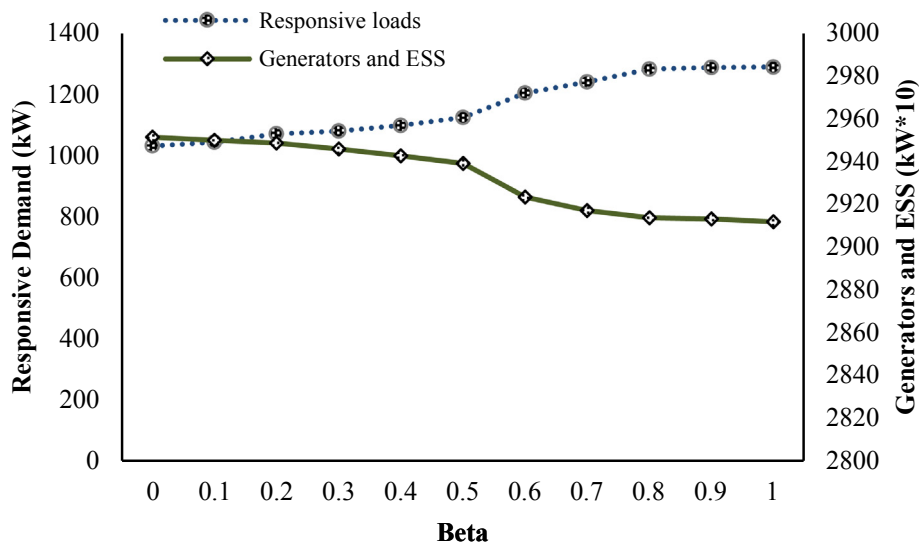


Fig. 16. Sensitivity of first- and second-stage energy scheduling decisions to risk-aversion parameter considering $r_t = 0\%$.

Table 7
Sensitivity of the MGO's first- and second-stage decision-making to the risk-aversion and reserve invoking parameters (First scenario).

Percentage of reserve invoking (r_t)	Reserve scheduling						Energy scheduling					
	$\sum_t R_t^{IL-RCI}$			$\sum_t R_{\omega,t}^{DG}$			$\sum_t (p_t^{IL-RCI} + p_t^{DN-RCI})$			$\sum_t (p_{\omega,t}^{DG} + p_{\omega,t}^{DCH})$		
	$\beta = 0$	$\beta = 0.3$	$\beta = 1$	$\beta = 0$	$\beta = 0.3$	$\beta = 1$	$\beta = 0$	$\beta = 0.3$	$\beta = 1$	$\beta = 0$	$\beta = 0.3$	$\beta = 1$
10%	1678.19	1666.90	1682.32	2485.21	2496.50	2481.08	980.26	984.70	1108.93	29600.45	29590.53	29476.17
30%	1536.06	1536.06	1536.06	2627.35	2627.35	2627.35	949.52	966.78	973.04	29713.73	29675.14	29666.20
70%	1251.39	1342.38	1332.32	2912.02	2821.03	2831.09	978.92	996.18	1024.285	29950.48	29811.02	29776.33
100%	177.07	304.09	151.85	3986.33	3859.32	4011.56	2022.71	1840.75	2074.03	28914.56	29091.94	28735.48

loads to decrease the difference between the worst and the best scenarios. This in turn leads to a lower CVaR.

Several aspects of the MG operation problem, including planning of standalone MGs in presence of uncertainties and modeling the cooperation between several MGs through clearing local energy and reserve markets deserve further investigation.

References

[1] Weber J, Heinrichs HU, Gillessen B, et al. Counter-intuitive behaviour of energy system models under CO2 caps and prices. *Energy* 2019;170:22–30.

[2] Cai W, Lai K, Liu C, et al. Promoting sustainability of manufacturing industry through the lean energy-saving and emission-reduction strategy. *Sci Total Environ* 2019;665:23–32.

[3] Lasseter RH. Smart distribution: coupled microgrids. *Proc IEEE* 2011;99:1074–82.

[4] Zheng Y, Jenkins BM, Kornbluth K, et al. Optimization of a biomass-integrated renewable energy microgrid with demand side management under uncertainty. *Appl Energy* 2018;230:836–44.

[5] Bahramara S, Golpīra H. Robust optimization of micro-grids operation problem in the presence of electric vehicles. *Sustain Cities Soc* 2018;37:388–95.

[6] Conti S, Nicolosi R, Rizzo S, et al. Optimal dispatching of distributed generators and storage systems for MV islanded microgrids. *IEEE Trans Power Deliv* 2012;27:1243–51.

[7] Elsieid M, Oukaour A, Gualous H, et al. Optimal economic and environment operation of micro-grid power systems. *Energy Convers Manag* 2016;122:182–94.

[8] Kanchev H, Colas F, Lazarov V, et al. Emission reduction and economical optimization of an urban microgrid operation including dispatched PV-based active generators. *IEEE Trans Sustain Energy* 2014;5:1397–405.

[9] Jiang Q, Xue M, Geng G. Energy management of microgrid in grid-connected and stand-alone modes. *IEEE Trans Power Syst* 2013;28:3380–9.

[10] Gupta A, Saini R, Sharma M. Modelling of hybrid energy system—Part II: combined dispatch strategies and solution algorithm. *Renew Energy* 2011;36:466–73.

[11] Morais H, Kádár P, Faria P, et al. Optimal scheduling of a renewable micro-grid in an isolated load area using mixed-integer linear programming. *Renew Energy* 2010;35:151–6.

[12] Ren H, Zhou W, Nakagami Ki, et al. Multi-objective optimization for the operation of distributed energy systems considering economic and environmental aspects. *Appl Energy* 2010;87:3642–51.

[13] Ashari M, Nayar C. An optimum dispatch strategy using set points for a photovoltaic (PV)–diesel–battery hybrid power system. *Sol Energy* 1999;66:1–9.

[14] Zhao B, Zhang X, Chen J, et al. Operation optimization of standalone microgrids considering lifetime characteristics of battery energy storage system. *IEEE Trans Sustain Energy* 2013;4:934–43.

[15] Oliveira D, de Souza AZ, Santos M, et al. A fuzzy-based approach for microgrids islanded operation. *Electr Power Syst Res* 2017;149:178–89.

[16] El-Bidairi KS, Nguyen HD, Jayasinghe S, et al. A hybrid energy management and battery size optimization for standalone microgrids: a case study for Flinders Island, Australia. *Energy Convers Manag* 2018;175:192–212.

[17] Cervantes I, Hernandez-Nochebuena M, Cano-Castillo U, et al. A graphical approach to optimal power management for uncertain OFF-Grid PV-FC-electrolyzer-battery hybrid systems. *Int J Hydrogen Energy* 2018;43:19336–51.

[18] Mazzola S, Vergara C, Astolfi M, et al. Assessing the value of forecast-based

dispatch in the operation of off-grid rural microgrids. *Renew Energy* 2017;108:116–25.

[19] Zhang Y, Fu L, Zhu W, et al. Robust model predictive control for optimal energy management of island microgrids with uncertainties. *Energy* 2018;164:1229–41.

[20] Tu T, Rajarathnam GP, Vassallo AM. Optimization of a stand-alone photovoltaic–wind–diesel–battery system with multi-layered demand scheduling. *Renew Energy* 2019;131:333–47.

[21] Razmi H, Doagou-Mojarrad H. Comparative assessment of two different modes multi-objective optimal power management of micro-grid: grid-connected and stand-alone. *IET Renew Power Gener* 2018. <https://doi.org/10.1049/iet-rpg.2018.5407>.

[22] Assaf J, Shabani B. Experimental study of a novel hybrid solar-thermal/PV-hydrogen system: towards 100% renewable heat and power supply to standalone applications. *Energy* 2018;157:862–76.

[23] Gupta R, Gupta NK. A robust optimization based approach for microgrid operation in deregulated environment. *Energy Convers Manag* 2015;93:121–31.

[24] Tabar VS, Ghassemzadeh S, Tohidi S. Energy management in hybrid microgrid with considering multiple power market and real time demand response. *Energy* 2019;174:10–23.

[25] Moradi H, Esfahanian M, Abtahi A, et al. Optimization and energy management of a standalone hybrid microgrid in the presence of battery storage system. *Energy* 2018;147:226–38.

[26] Alharbi W, Raahemifar K. Probabilistic coordination of microgrid energy resources operation considering uncertainties. *Electr Power Syst Res* 2015;128:1–10.

[27] Rathore A, Patidar N. Reliability assessment using probabilistic modelling of pumped storage hydro plant with PV-Wind based standalone microgrid. *Int J Electr Power Energy Syst* 2019;106:17–32.

[28] Farsangi AS, Hadyeghparast S, Mehdinejad M, et al. A novel stochastic energy management of a microgrid with various types of distributed energy resources in presence of demand response programs. *Energy* 2018;160:257–74.

[29] Wang MQ, Gooi HB. Spinning reserve estimation in microgrids. *IEEE Trans Power Syst* 2011;26:1164–74.

[30] Tenfen D, Finardi EC. A mixed integer linear programming model for the energy management problem of microgrids. *Electr Power Syst Res* 2015;122:19–28.

[31] Nguyen DT, Le LB. Risk-constrained profit maximization for microgrid aggregators with demand response. *IEEE Trans Smart Grid* 2015;6:135–46.

[32] Gerard H, Puente EIR, Six D. Coordination between transmission and distribution system operators in the electricity sector: a conceptual framework. *Util Pol* 2018;50:40–8.

[33] Conejo AJ, Carrión M, Morales JM. Decision making under uncertainty in electricity markets. Springer US; 2010.

[34] Sheikhhamedi P, Bahramara S, Moshtagh J, et al. A risk-based approach for modeling the strategic behavior of a distribution company in wholesale energy market. *Appl Energy* 2018;214:24–38.

[35] Shen J, Jiang C, Liu Y, et al. A microgrid energy management system and risk management under an electricity market environment. *IEEE Access* 2016;4:2349–56.

[36] Logenthiran T, Srinivasan D, Khambadkone AM. Multi-agent system for energy resource scheduling of integrated microgrids in a distributed system. *Electr Power Syst Res* 2011;81:138–48.

[37] In-Su B, Jin OK, Jae-Chul K, et al. Optimal operating strategy for distributed generation considering hourly reliability worth. *IEEE Trans Power Syst* 2004;19:287–92.